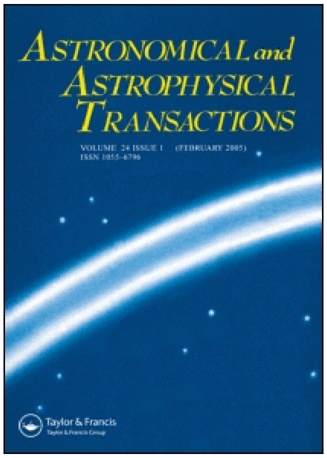

Astronomical & Astrophysical Transactions
The Journal of the Eurasian Astronomical Society
Publication details, including instructions for authors and subscription information:
http://www.informaworld.com/smpp/title~content=t713453505

Orbits in disc galaxies with rapidly rotating massive nuclei: comparison with data from observations

N. J. Papadopoulos [a]; N. D. Caranicolas [a]
[a] Department of Physics, Section of Astrophysics, Astronomy and Mechanics, University of Thessaloniki, Thessaloniki, Greece

Online Publication Date: 01 January 2005
To cite this Article: Papadopoulos, N. J. and Caranicolas, N. D. (2005) 'Orbits in disc galaxies with rapidly rotating massive nuclei: comparison with data from observations', Astronomical & Astrophysical Transactions, 24:3, 241 - 252
To link to this article: DOI: 10.1080/10556790500513620
URL: http://dx.doi.org/10.1080/10556790500513620

Astronomical and Astrophysical Transactions
Vol. 24, No. 3, June 2005, 241–252

Orbits in disc galaxies with rapidly rotating massive nuclei: comparison with data from observations

N. J. PAPADOPOULOS and N. D. CARANICOLAS*

Department of Physics, Section of Astrophysics, Astronomy and Mechanics,
University of Thessaloniki, 541 24 Thessaloniki, Greece

(Received 14 September 2005)

An axially symmetric galactic dynamic model is used, with a disc, a massive nucleus and halo components, in order to reproduce recently obtained observation data in disc galaxies. The model reproduces very well two basic physical quantities, i.e. the high-velocity rotation and the high surface mass density in the central regions of some galaxies such as the galaxy NGC 3079. Going a step further, we investigate the properties of orbits in the model, the behaviour of the velocities of the system and their connections with the value of the conserved L_z component of the angular momentum. The regular or chaotic nature of motion is also studied. All the above studies are made in two different cases: firstly, when the model is time independent and, secondly, when the model evolves with time.

Keywords: Orbits; Disc galaxies; Dense nucleus; Galactic models

1. Introduction

Dynamic searches indicate the presence of massive objects in the central regions of galaxies such as M31, M87 and NGC 4594. The estimation for the central masses are from $10^6 M_\odot$ up to about $10^{10} M_\odot$. Improved ground-based instruments and especially the Hubble Space Telescope have given interesting information on the subject. Dynamic evidence for the presence of a massive object in the cores of galaxies is based on the value of the mass-to-luminosity ratio M/L. If M/L increases towards the centre to values that are several times larger than normal, this strongly indicates that a massive object has been discovered [1]. Rapid rotation is also a strong indicator for the presence of a massive object [2–6].

In the present article we use the simple dynamic model given by the potential

$$V_{\mathrm{tot}}(r,z) = -\frac{M_\mathrm{n}}{(r^2+z^2+c_\mathrm{n}^2)^{1/2}} - \frac{M_\mathrm{d}}{\{r^2+[\alpha+(z^2+h^2)^{1/2}]^2\}^{1/2}} - \frac{M_\mathrm{h}}{(r^2+z^2+c_\mathrm{h}^2)^{1/2}}, \tag{1}$$

*Corresponding author. Email: caranic@astro.auth.gr

Astronomical and Astrophysical Transactions
ISSN 1055-6796 print/ISSN 1476-3540 online © 2005 Taylor & Francis
http://www.tandf.co.uk/journals
DOI: 10.1080/10556790500513620

where r, φ, z are the cylindrical coordinates. Equation (1) describes motion in an axially symmetric disc galaxy with a nucleus and a halo component. Here M_n, M_d and M_h are the masses of the nucleus, disc and halo respectively, α is the disc scale length, h is the disc scale height, and c_n and c_h represent the scale lengths of the nucleus and halo, respectively.

The main targets of this paper are, firstly, to use this model in order to reproduce analytically some physical properties such as the rotational velocity and density and to compare the results with the outcomes coming from observations and, secondly, to investigate, numerically, the character of motion (regular or chaotic) and to find connections between the nature of motion and the above physical quantities. We shall start from the time-independent model and then we shall consider the evolving model. In this latter model an exponential mass transportation is taking place from the halo to the disc and the nucleus simultaneously.

In our numerical and analytical calculations the well-known system of galactic units is used where the unit of length is 1 kpc, the unit of time is $0.977\,46 \times 10^8$ year and the unit of mass is $2.325 \times 10^7 M_\odot$. The velocity unit is $10\,\mathrm{km\,s^{-1}}$ while G is equal to unity. In the above units we use the values $\alpha = 3\,\mathrm{kpc}$, $h = 0.2\,\mathrm{kpc}$, $c_\mathrm{n} = 0.1\,\mathrm{kpc}$ and $c_\mathrm{h} = 10\,\mathrm{kpc}$. We consider a system with a fixed value of total mass; thus we take $M_\mathrm{n} + M_\mathrm{d} + M_\mathrm{h} = 12\,000$.

2. Analytical and seminumerical results

In this section, we shall use the model to derive and study the properties of several physical quantities such as the rotational velocity and mass density. Figure 1(a) shows the rotational velocity Θ versus the radius r in the central region of the model. The values of the parameters are $M_\mathrm{n} = 600$, $M_\mathrm{h} = 2000$ and $M_\mathrm{d} = 9400$. In figure 1(b) a plot of Θ versus M_n is shown, when $r_\mathrm{o} = 0.2\,\mathrm{kpc}$, $M_\mathrm{h} = 2000$, while $M_\mathrm{d} = 12\,000 - M_\mathrm{h} - M_\mathrm{n}$. Observing these figures, one can derive two basic conclusions.

(i) In galaxies with massive central concentrations the rotational velocity is and remains high near the centre.
(ii) The more massive the nucleus, the higher is Θ.

It is important that the above results are in agreement with the observational data obtained by Sofue *et al.* [6, 7] for disc galaxies with massive nuclei.

It is of interest to see what happens with the mass density in the central regions of the model. Figure 2 shows the surface mass density (SMD) (in $M_\odot$ per square parsec) in the galactic plane ($z = 0$) as a function of the radius r. As can be seen, the SMD in the central 100 pc region is of the order of $100\,000 M_\odot\,\mathrm{pc}^{-2}$ or more. This value is in agreement with the value of the SMD for the disc galaxy NGC 3079 derived recently by Sofue *et al.* [6] using observational data. Thus, we can conclude that the observed SMD is close to the value of the SMD obtained from our model.

Indeed the SMD is connected to the mass density $\rho(r, z)$ through the relation

$$\mathrm{SMD} = \int_0^z \rho(r, z)\,\mathrm{d}z. \tag{2}$$

In the galactic plane the mass density becomes $\rho(r, 0)$ and equation (2) yields

$$\mathrm{SMD} = \int_0^z \rho(r, 0)\,\mathrm{d}z = 1000\rho(r, 0), \tag{3}$$

where we have choosen 1 kpc for the disc height. The plot in figure 2 is from equation (3) where the mass densities $\rho(r, z)$ and $\rho(r, 0)$ are found from the potential (1) using the Poisson equation.

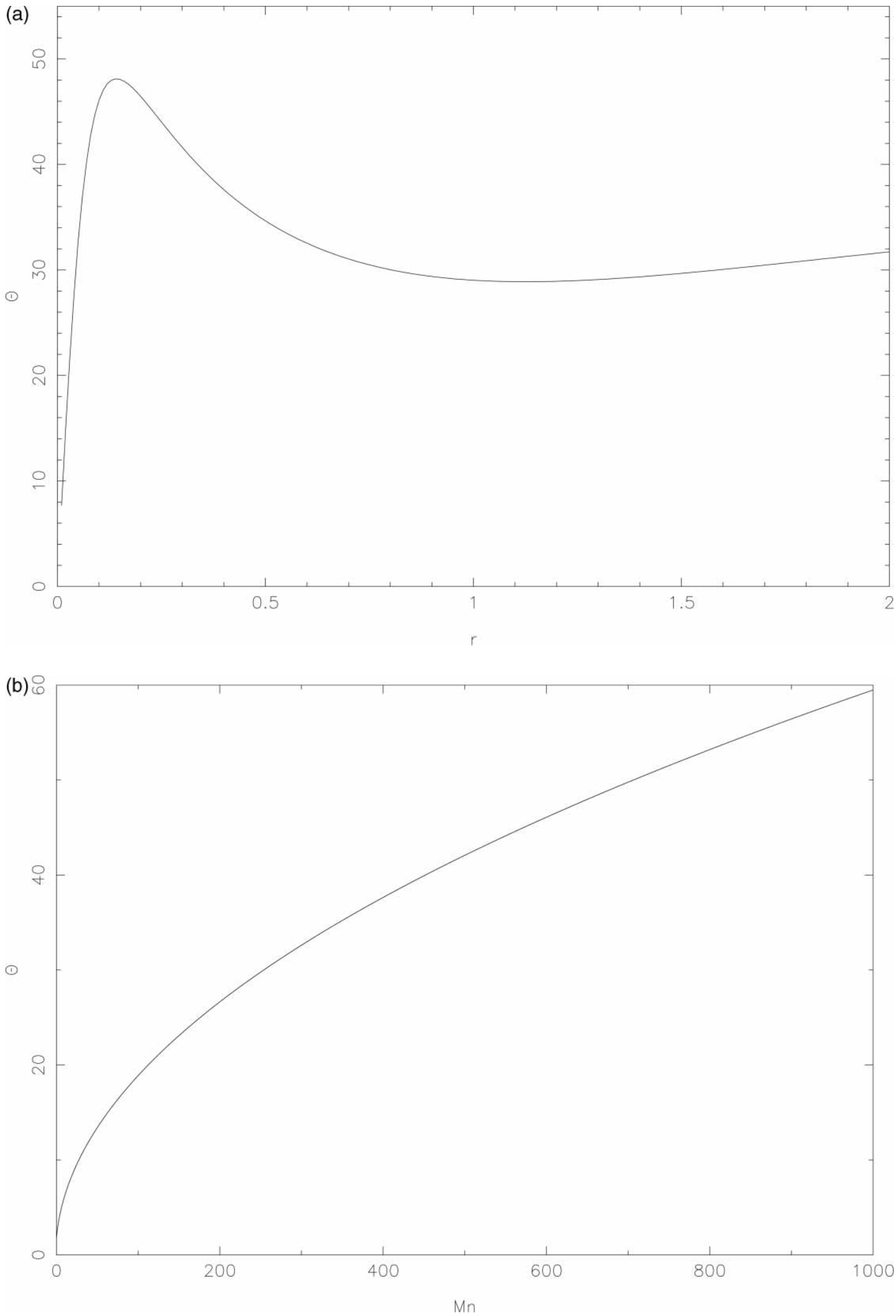

Figure 1. (a) Rotational velocity Θ *vs* radius r in the central region of the model. The values of the parameters are given in text. (b) Rotational velocity Θ *vs* M_{n} in the central region of the model. The values of the parameters are given in text.

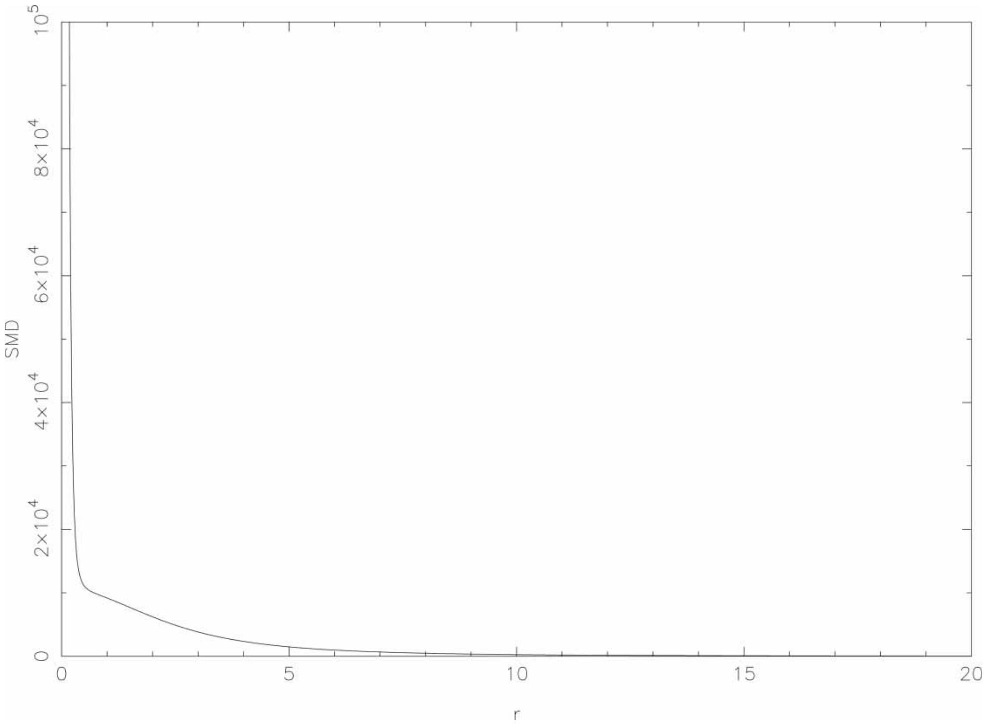

Figure 2. The SMD (in $M_\odot$ per square parsec) in the galactic plane ($z = 0$) as a function of the radius r.

Using the conserved L_z component of the angular momentun we can deal with a two-dimensional problem described by the Hamiltonian

$$H = \frac{1}{2}(p_r^2 + p_z^2) + V_{\mathrm{eff}}(r, z) = E, \tag{4}$$

where p_r and p_z are the momenta, per unit mass, conjugate to r and z, respectively,

$$V_{\mathrm{eff}} = \frac{L_z^2}{2r^2} + V(r, z), \tag{5}$$

is the effective potential and E is the numerical value of the Hamiltonian which coincides with the total energy of the test particle. The Hamiltonian (4) describes the motion in the r–z meridian plane rotating at the angular velocity

$$\dot{\phi} = \omega = \frac{L_z}{r^2}. \tag{6}$$

In order to visualize the properties of orbits and the nature (regular or chaotic) of motion, we use the r–p_r, $z = 0$, $p_z>0$, Poincaré phase plane. This plane is found using the numerical integration of the equations of motion

$$\ddot{r} = -\frac{\partial V_{\mathrm{eff}}}{\partial r}, \quad \ddot{z} = -\frac{\partial V_{\mathrm{eff}}}{\partial z}. \tag{7}$$

Before carrying out numerical integration let us present some more semianalytical results. Setting $z = p_z = 0$ in equation (4) we obtain the limiting curve in the r–p_r phase plane (i.e. the curve containing all the invariant curves for a given value of the energy integral E):

$$\frac{1}{2}p_r^2 + V_{\text{eff}}(r) = E. \tag{8}$$

The maximum value of the velocity p_r (momentun per unit mass) on the limiting curve can give us a measure of the total velocity in the r–p_r phase plane, as in the limiting curve $p_z = 0$. If we set $p_r = \upsilon$ in equation (8) we find that

$$\frac{1}{2}\upsilon^2 = E - \frac{L_z^2}{2r^2} - V(r). \tag{9}$$

It is evident that, for a given value of L_z, υ becomes a maximum if V_{eff} is a minimum. However, for the minimun of V_{eff} we must have

$$\frac{L_z^2}{r^3} = \frac{\partial V(r)}{\partial r}. \tag{10}$$

Solving equations (9) and (10) simultaneously we can find a relationship between $\upsilon_{\max}$ and L_z, this relationship is shown in figure 3. We see that the maximum velocity decreases exponentially as L_z increases. We shall come to this point again in the next section.

3. Numerical results for the time-independent potential

Figure 4(a) shows the $r - p_r$ Poincaré phase plane when $L_z = 5$, $M_{\text{n}} = 400$, $M_{\text{h}} = 0$ and $M_{\text{d}} = 11\,600$. The value of energy is $E = -850$. Two interesting comments can be made. The first is that a large part of the phase plane is covered by chaotic orbits and the second is that, at small radii, near the centre of the system, the velocity reaches high values, of the order of $1000\,\text{km s}^{-1}$. Figure 4(b) is same as figure 4(a) but for $L_z = 20$. Here, the situation looks

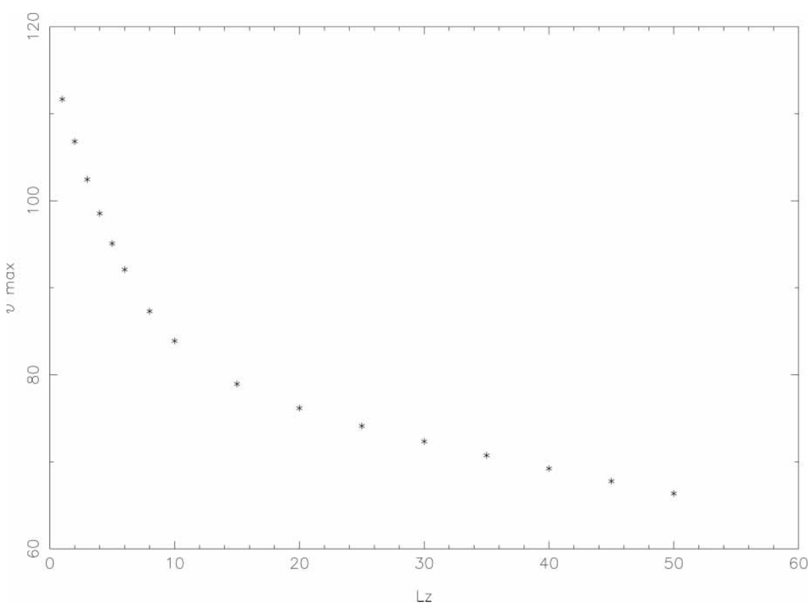

Figure 3. Relationship between $\upsilon_{\max}$ and L_z. The maximum velocity decreases exponentially as L_z increases.

different. The chaotic region is very small while the velocities in the central region are half those observed in figure 4(a). Thus, we can conclude that, in disc galaxies with high and dense central concentrations, low-angular-momentum stars are in chaotic motion and this chaotic motion occurs at high velocities reaching 1000 km s^{-1} in the central regions. On the contrary, at

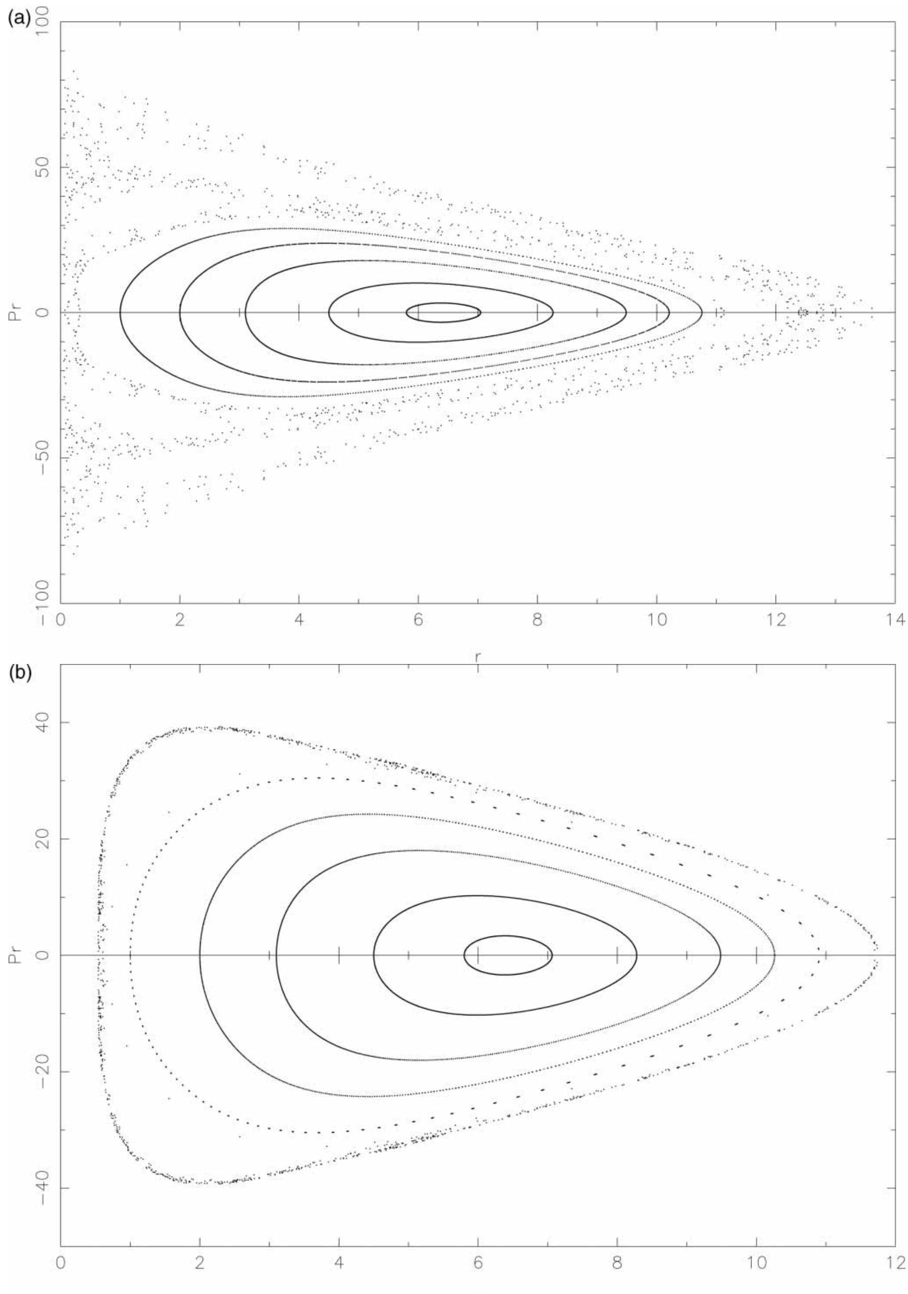

Figure 4. (a) The $r - p_r$ Poincare phase plane when $L_z = 5$, $M_n = 400$, $M_h = 0$, while $M_d = 11\,600$. The value of energy is $E = -850$. Note that the velocity reaches high values, of order of 1000 km/s. (b) The $r - p_r$ Poincare phase plane when $L_z = 20$, $M_n = 400$, $M_h = 0$, while $M_d = 11\,600$. Note that the chaotic region is very small while the velocities in the central region are also small.

large galactocentric distances the chaotic motion occurs at small velocities. On the other hand, we clearly see that, as the angular momentum increases, we immediately observe significant decreases in the number of chaotic regions and also in the total velocity.

It is very important to note that the above results from numerical integration of the equations of motion are in agreement with the semianalytical or seminumerical results presented in section 2. This strongly suggests that low-angular-momentum stars are old population II stars that cross with high velocities the galactic plane near the nucleus and consequently they reach significantly large z heights [8]. On the contrary, high-angular-momentum stars stay near the galactic plane; therefore they must be population I stars.

4. The evolving model

We can now see what happens in the case when the galaxy evolves with time. For simplicity we assume that the total mass of the galaxy remains constant while we have exponential mass transportation from the halo to the disc and the nucleus simultaneously. The transportation equations are written

$$M_{\mathrm{h}}(t) = M_{\mathrm{hi}} - m_1[1 - \exp(-kt)], \tag{11}$$

$$M_{\mathrm{d}}(t) = M_{\mathrm{di}} + (m_1 - m_2)[1 - \exp(-kt)], \tag{12}$$

$$M_{\mathrm{n}}(t) = M_{\mathrm{ni}} + m_2[1 - \exp(-kt)], \tag{13}$$

where M_{hi}, M_{di} and M_{ni} are the initial masses of the halo, disc and nucleus respectively while $M_{\mathrm{h}}(t)$, $M_{\mathrm{d}}(t)$ and $M_{\mathrm{n}}(t)$ are the masses of the halo, disc and nucleus respectively at time t; m_1 is the portion of the halo mass that is transported, m_2 is the mass that goes to the nucleus and $m_1 - m_2$ is the mass that goes to the disc; $k > 0$ is a parameter. Note that the total mass of the galaxy is fixed so that $M_{\mathrm{n}}(t) + M_{\mathrm{d}}(t) + M_{\mathrm{h}}(t) = 12\,000$.

Now equation (9) is a function of time and is given by

$$\frac{1}{2}v(t)^2 = E - \frac{L_z^2}{2r^2} - V(r,t). \tag{14}$$

Figure 5 shows the evolution of the velocity with the time, derived using equation (14), at a fixed point near the centre, $r = r_0 = 0.2\,\mathrm{kpc}$, $z = 0$, when $E = -500$ and $L_z = 5$. Here we take $M_{\mathrm{hi}} = 10\,900$, $M_{\mathrm{di}} = 1095$, $M_{\mathrm{ni}} = 5$, $k = 0.01$, $m_1 = 10\,900$ and $m_2 = 995$. The velocity increases exponentially as mass is transported from the halo to the disc and nucleus. Note that after the end of the mass transportation the velocity remains constant.

In figure 6, one can see the evolution of the mass density ρ with the time in $M_\odot$ per cubic parsec.

The mass density was found using the Poisson equation

$$\nabla^2 V(r,t) = 4\pi G(r,t) \tag{15}$$

for the evolving model. The values of the parameters are as in figure 5. One can see that the value of the mass density increases rapidly as mass is transported from the halo to the disc and nucleus and remains constant after the end of the mass transportation.

Figure 7 shows the evolution of the velocity with time found using numerical integration. The orbit started at $r = r_0 = 0.2\,\mathrm{kpc}$, $z = 0$, with the initial value of energy $E = -500$, while the value of the initial total (vertical) velocity was found using the initial value of the energy integral. All other parameters are as in figure 5 and $k = 0.001$. As indicated by

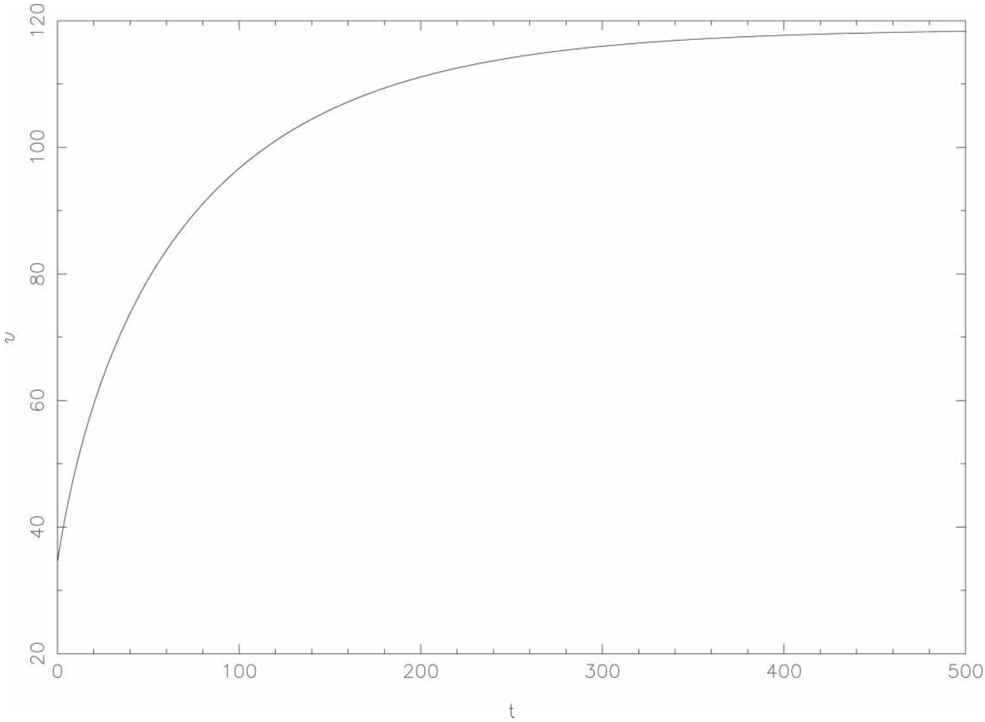

Figure 5. Evolution of the velocity with time at a fixed point near the centre. The values of the parameters are given in the text.

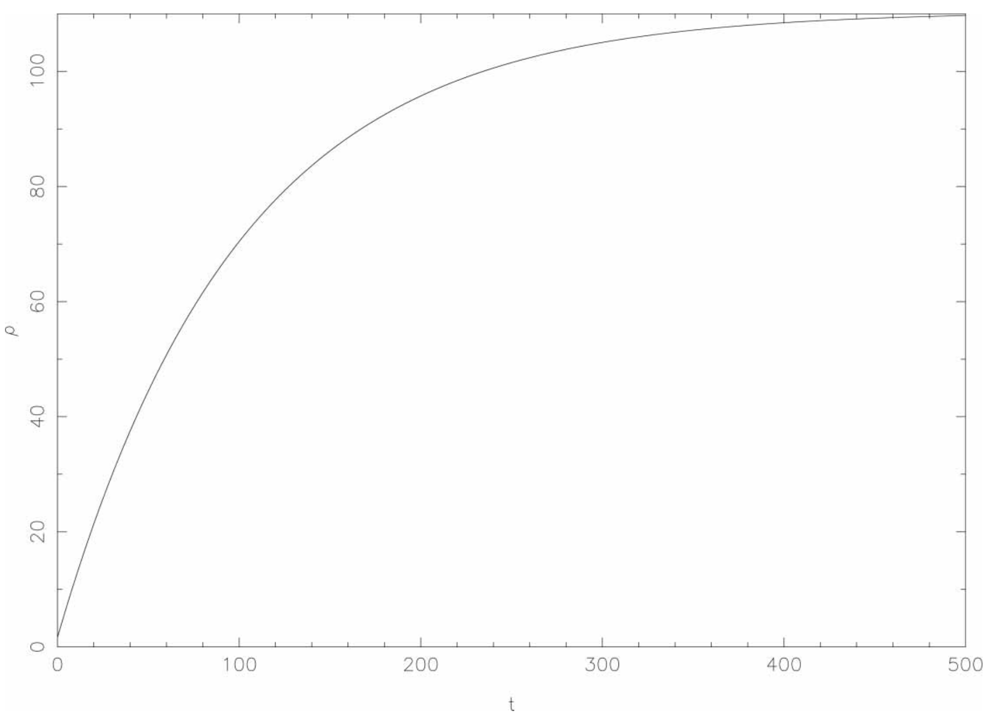

Figure 6. Evolution of the mass density ρ with time at a fixed point near the centre. The values of the parameters are as in figure 5.

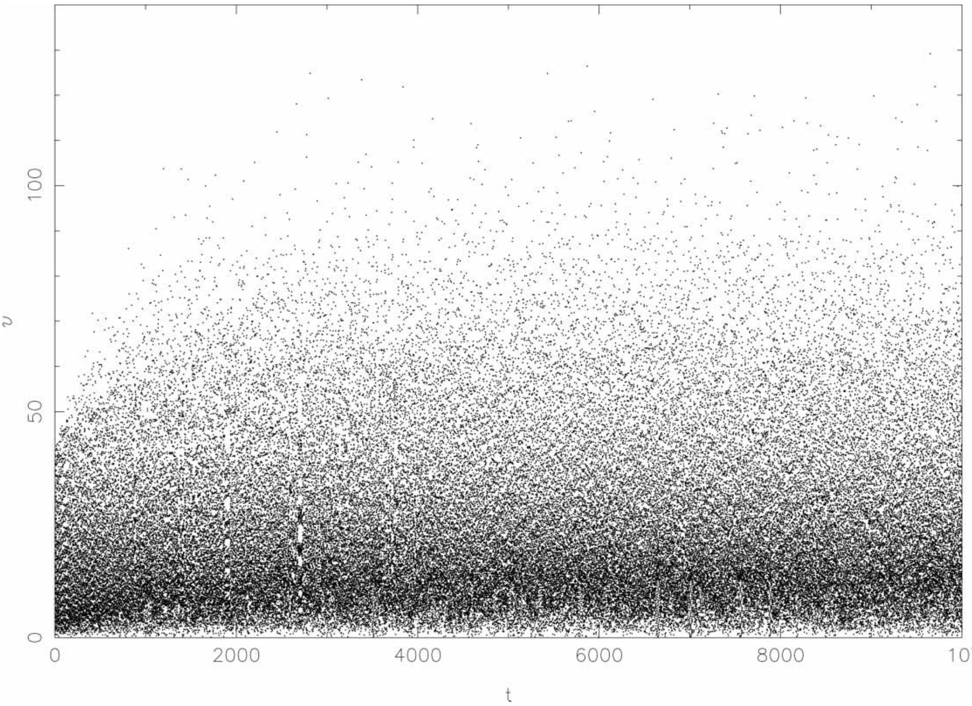

Figure 7. Same as figure 5, found using numerical integration. The motion is chaotic.

the Lyapunov characteristic number (LCN) [9] shown in figure 8, the orbit is chaotic. It is interesting to observe what happens to the star's velocity during the mass transportation described by equations (11)–(13). We see that the star's velocity can reach high values up to 1300 km s^{-1} but only for short time periods. Most of the time the star travels at velocities lower than 500 km s^{-1}. A large number of chaotic orbits were calculated and the behaviour is similar to that shown in figure 7. From a statistical point of view this means that a small number of stars reach these high velocities while the majority of stars travel at much lower velocities. Figure 9 shows the evolution of a regular orbit as indicated by the LCN shown in figure 10. The initial conditions are $r = r_0 = 3.0$ kpc, $z = 0$, with an initial value of energy $E = -500$, while the value of the initial total (vertical) velocity was found using the initial value of the energy integral. Here, we see that the maximum velocity is of the order of 600 km s^{-1} while there are short time periods when the star travels at very low velocities, less than 100 km s^{-1}. What is strongly suggested by the velocity versus time plot in an evolving system is that stars in chaotic orbits can reach high velocities while, when they are in regular motion, the maximum velocity is half that. The number of stars reaching high velocities (above 1000 km s^{-1}) or low velocities (less than 100 km s^{-1}) is small.

It is interesting to note that the orbits shown in figures 7 and 9 are orbits with the same parameters and only different initial conditions. This means that stars with the same physical parameters and with the same initial value of energy can travel in regular or chaotic orbits depending strongly on the initial conditions. Of course this is not a new result. What is interesting is that, in an evolving model, stars with the same parameters and only with different starting points (the initial velocity obtained from the initial value of the energy integral) can display high or low velocities. The high velocities are displayed when the stars are in a chaotic orbit while, when the orbits are regular, the velocities are much lower.

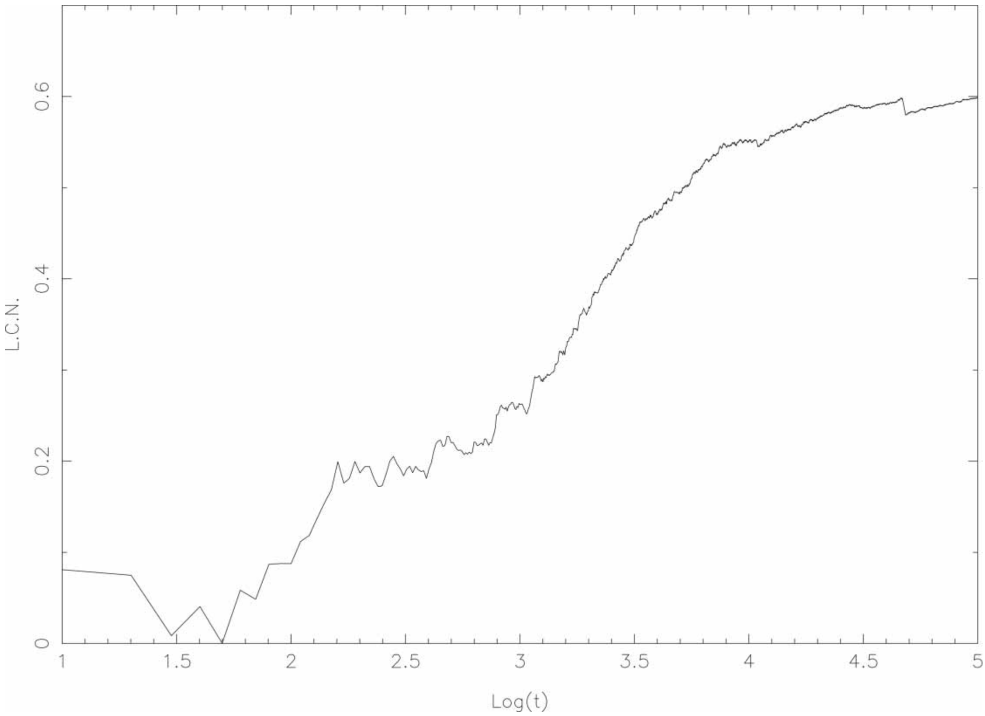

Figure 8. LCNs for the orbit of figure 7.

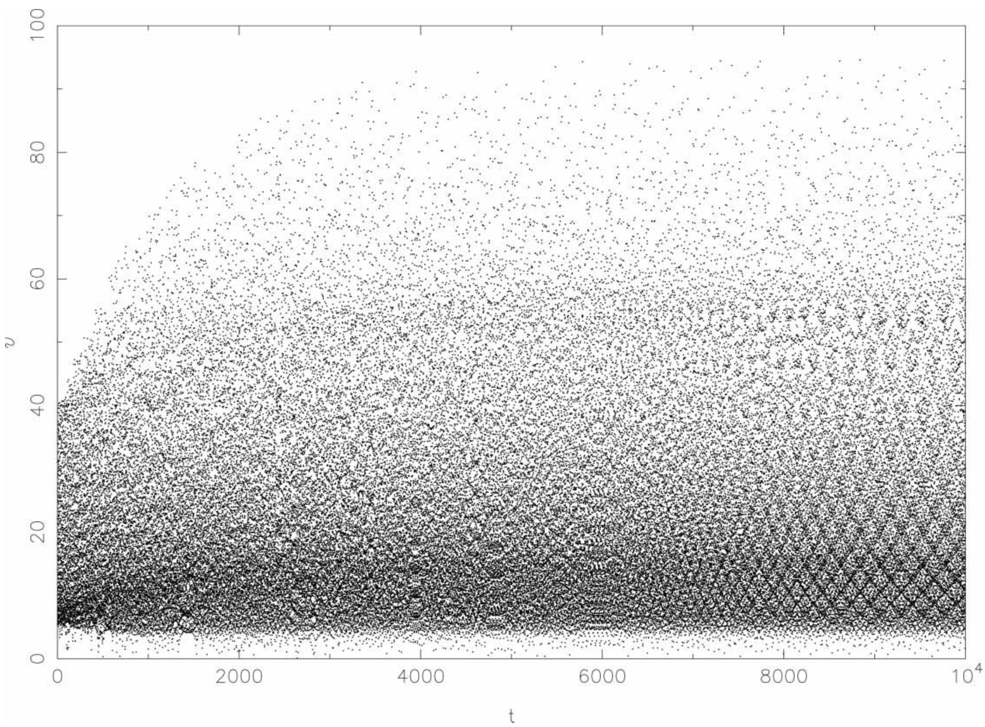

Figure 9. Same as figure 7 for a regular orbit.

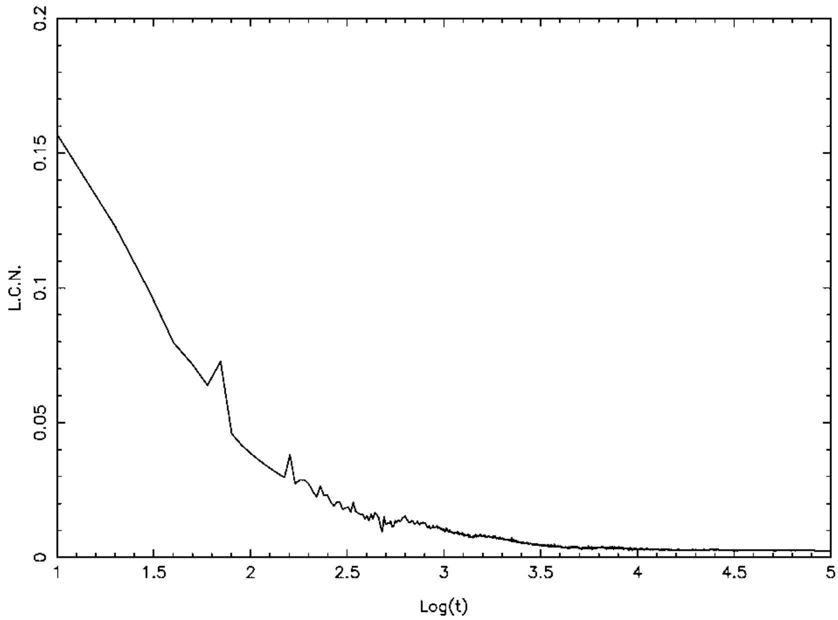

Figure 10. LCNs for the orbit of figure 9.

5. Discussion and conclusions

In the present paper, we have used an axially symmetric galactic dynamic model, with a disc, a massive nucleus and halo components, in order to study and follow the evolution of some physical quantities such as the rotational velocity and mass density in the central regions of the model. Furthermore, we have investigated the properties of orbits in the model, the behaviour of the velocities of the system and their connections to the value of the conserved L_z component of the angular momentum. Our results lead to the following suggestions.

(1) In galaxies with massive cores the rotational velocity is and remains high near the centre. The more massive the nucleus, the higher is the rotational velocity. The results from the model are in agreement with the observational data obtained by Sofue *et al.* [6, 7] for disc galaxies with massive central concentrations.
(2) The SMD in the galactic plane in the central 100 pc region is of the order of $1000 M_\odot\,\mathrm{pc}^{-2}$ or more. This value is in complete agreement with the value of surface density for the disc galaxy NGC 3079 derived recently by Sofue *et al.* [6] using observational data. On this basis, one can conclude that the observed SMD is in agreement with the value of the SMD from our model.
(3) Our numerical experiments show that, at small radii, near the centre of the model, when the angular momentum is low (say $L_z \leq 5$), the velocity reaches high values, of the order of $1000\,\mathrm{km\,s^{-1}}$. For higher values of the angular momentum the chaotic region decreases while the velocities in the central region are lower. This shows that, in disc galaxies with high and dense central concentrations, low-angular-momentum stars are in chaotic motion and this chaotic motion occurs at high velocities reaching $1000\,\mathrm{km\,s^{-1}}$ in the central regions. At large galactocentric distances the chaotic motion occurs at low velocities.
(4) As the angular momentum increases, we immediately observe significant decreases in the number of chaotic regions and in the total velocity as well.

(5) In the evolving model the velocity and density increase exponentially as mass is transported from the halo to the disc and nucleus (see also [10]).
(6) Numerical calculations suggest that, in an evolving model, stars with the same parameters and only with different starting points (the initial velocity obtained using the initial value of the energy integral) can display high or low velocities. The high velocities are displayed when the stars are in chaotic orbits while, when the orbits are regular, the velocities are much lower. The number of stars reaching high velocities (above $1000\,\mathrm{km\,s^{-1}}$) or low velocities (less than $100\,\mathrm{km\,s^{-1}}$) is small.

References

[1] J. Kormedy and D. Richstone, A. Rev. Astron. Astrophys. **33** 581 (1995).
[2] M. Miyoshi, J. Moran, J. Herstein *et al.*, Nature **373** 127 (1995).
[3] L.J. Greenhill and C. Gwinn, Astrophys. Space Sci. **248** 261 (1997).
[4] V. Rubin, J.D.P. Kenney and J.S. Young, Astron. J. **113** 1250 (1997).
[5] F. Bertola, M. Cappellari, J.G. Funes *et al.*, Astrophys. J. **509** L93 (1998).
[6] Y. Sofue, J. Koda, H. Naganishi *et al.*, *Proceedings of the Japan–German Seminar* (Sendai, Japan, 2001) pp. 171.
[7] Y. Sofue, Y. Tutui, M. Homma *et al.*, Astrophys. J. **523** 136 (1999).
[8] N.D. Caranicolas and K.A. Innanen, Astron. J. **102** 1343 (1991).
[9] A.J. Lichtenberg and M.A. Lieberman, *Regular and Stochastic Motion* (Springer, Berlin, 1983).
[10] N.D. Caranicolas and N.J. Papadopoulos, Astron. Astrophys. **399** 957 (2003).